



Structure Activity Relationship of *N*-Substituted Phenylhydrazolones Against *Trypanosoma cruzi* Amastigotes

Maarten Sijm¹, Louis Maes², Iwan J. P. de Esch¹, Guy Caljon², Geert Jan Sterk¹ and Rob Leurs^{1*}

¹Division of Medicinal Chemistry, Faculty of Sciences, The Amsterdam Institute of Molecular and Life Sciences (AIMMS), Vrije Universiteit Amsterdam, Amsterdam, Netherlands, ²Laboratory for Microbiology, Parasitology and Hygiene (LMPH), University of Antwerp, Antwerp, Belgium

OPEN ACCESS

Edited by:

Gildardo Rivera,
Instituto Politécnico Nacional (IPN),
Mexico

Reviewed by:

Gabriella Gabriella,
University of Florence, Italy
Guillermo R. Labadie,
National University of Rosario,
Argentina
Andrei I. Khlebnikov,
Tomsk Polytechnic University, Russia

*Correspondence:

Rob Leurs
r.leurs@vu.nl

Specialty section:

This article was submitted to
Medicinal and
Pharmaceutical Chemistry,
a section of the journal
Frontiers in Chemistry

Received: 20 September 2020

Accepted: 16 April 2021

Published: 30 April 2021

Citation:

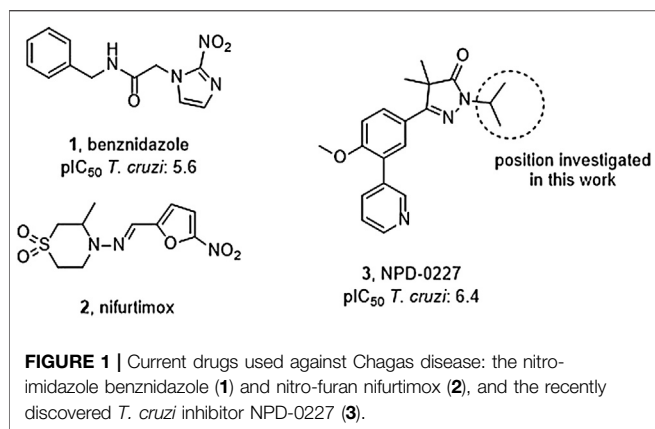
Sijm M, Maes L, de Esch IJP, Caljon G,
Sterk GJ and Leurs R (2021) Structure
Activity Relationship of *N*-Substituted
Phenylhydrazolones Against
Trypanosoma cruzi Amastigotes.
Front. Chem. 9:608438.
doi: 10.3389/fchem.2021.608438

Current drugs for Chagas disease have long treatment regimens with occurrence of adverse drug effects leading to poor treatment compliance. Novel and efficacious medications are therefore highly needed. We previously reported on the discovery of NPD-0227 (2-isopropyl-5-(4-methoxy-3-(pyridin-3-yl)phenyl)-4,4-dimethyl-2,4-dihydro-3H-pyrazol-3-one) as a potent *in vitro* inhibitor of *Trypanosoma cruzi* (pIC₅₀ = 6.4) with 100-fold selectivity over human MRC-5 cells. The present work describes a SAR study on the exploration of substituents on the phenylpyrazolone nitrogen. Modifications were either done directly onto this pyrazolone nitrogen or alternatively by introducing a piperidine linker. Attention was pointed toward the selection of substituents with a cLogP preferably below NPD-0227's cLogP of 3.5. Generally the more apolar compounds showed better activities than molecules with cLogPs <2.0. Several new compounds were identified with potencies that are in the same range as NPD-0227 (pIC₅₀ = 6.4) and promising selectivities. While the potency could not be improved, valuable SAR was obtained. Furthermore the introduction of a piperidine linker offers new opportunities for derivatization as valuable novel starting points for future *T. cruzi* drug discovery.

Keywords: structure activity relationship, chagas disease, phenotypic optimization, trypanosoma cruzi, phenylpyrazolones

INTRODUCTION

The protozoan parasite *Trypanosoma cruzi* is the causative agent of Chagas disease. It is estimated that over six million people are infected worldwide, the majority in Latin-America where the parasite is endemic. (Lidani et al., 2019; WHO, 2021). *T. cruzi* is spread by several insect vectors, most of which belong to the triatomine family (Kollien and Schaub, 2000; Martinez et al., 2019). Other ways of transmission are *via* blood transfusions, laboratory accidents or parental transmission from mother to infant (Schmunis, 1999; Torrico et al., 2004; Rassi et al., 2010). The life cycle of *T. cruzi* consists of several developmental stages in the mammalian host and insect vector (Rassi et al., 2010). While the vector appears unaffected by the parasite, infected humans can develop life-threatening symptoms and pathologies. The acute stage of the disease starts shortly after the parasite enters the body but a strong immune response will cause a large reduction of the initial peak of parasitemia, however, without full elimination of the parasite leading to persistent infection of certain tissues



(Dias, 1984). The acute symptoms are non-specific, such as fever, mild splenomegaly and edema, making diagnosis difficult (Prata, 2001). After 2 months, the disease enters the chronic phase in which the parasite becomes dormant and no symptoms are observed. This dormant phase can last for over 10 years up to lifelong (Prata, 2001). Estimates of further evolution of chronic infection toward clinical symptoms, such as cardiopathy or megaesophagus and megacolon, ranges between 10–60% of infected people and varies widely in different regions (Coura and Viñas, 2010; Coura and Borges-Pereira, 2011). Patients can become life-long asymptomatic carriers thus representing a parasite reservoir.

Vector control, early diagnosis and effective chemotherapy are essential to combat Chagas disease. Two drugs are currently marketed: the nitro-imidazole benznidazole (**1**, **Figure 1**) and the nitro-furan nifurtimox (**2**) (Rassi et al., 2010). Both drugs contain a nitro-aromatic functionality which is commonly associated with toxic side effects. Furthermore, the treatment regimens of both vary between 60–90 days and are known to cause various side effects which cause patients to discontinue

their treatment (Castro et al., 2006; Pinazo et al., 2013). Benznidazole (**1**) is currently used as first-line treatment as it has a better overall safety profile (Alpern et al., 2017). While the efficacy of both drugs is well established in the acute phase, much debate is ongoing on about their efficacy in the chronic phase (Sgambatti de Andrade et al., 1996; Zhang and Tarleton, 1999; Bern, 2011). The recent BENEFIT trial investigated the efficacy of Benznidazole (**1**) on chronic Chagas' heart disease. While reduced parasitemia was observed by PCR, this did not result in significant reduction of clinical deterioration of cardiac function after 5 years (Morillo et al., 2015). Afterward several concerns were raised in literature with regard to the PCR analysis and benznidazole dosage, precluding firm conclusions on the efficacy potential in the chronic phase of infection (Hamers et al., 2016).

The overall need for new and improved chemotherapies for Chagas disease is high, both for current and future patients. New medication is also needed as contingency measure for upcoming resistance against the available current drugs (Coura and Viñas, 2010; Mejia et al., 2012). Unfortunately, the pipeline toward new drugs is largely empty. Most research on *T. cruzi* is performed in academia though the last few years several public-private collaborations have been initiated. In this paper, we describe part of the research of the EU-funded, public-private consortium PDE4NPD, that focuses on 3'5'-cyclic nucleotide phosphodiesterases (PDEs) as targets against several neglected tropical diseases. The present work further elaborates the SAR of the previously reported *T. cruzi* inhibitor NPD-0227 (**3**, **Figure 1**) and investigates the role of different substituents on the pyrazolone nitrogen (Sijm et al., 2019). Besides the SAR aiming at improving potency, compounds were also specifically designed to improve physicochemical properties, such as cLogP and solubility. As *T. cruzi* ultimately proceeds *via* a dormant intracellular form, a possible drug needs to pass several cell membranes before reaching the parasite. During this process the drug is transferred

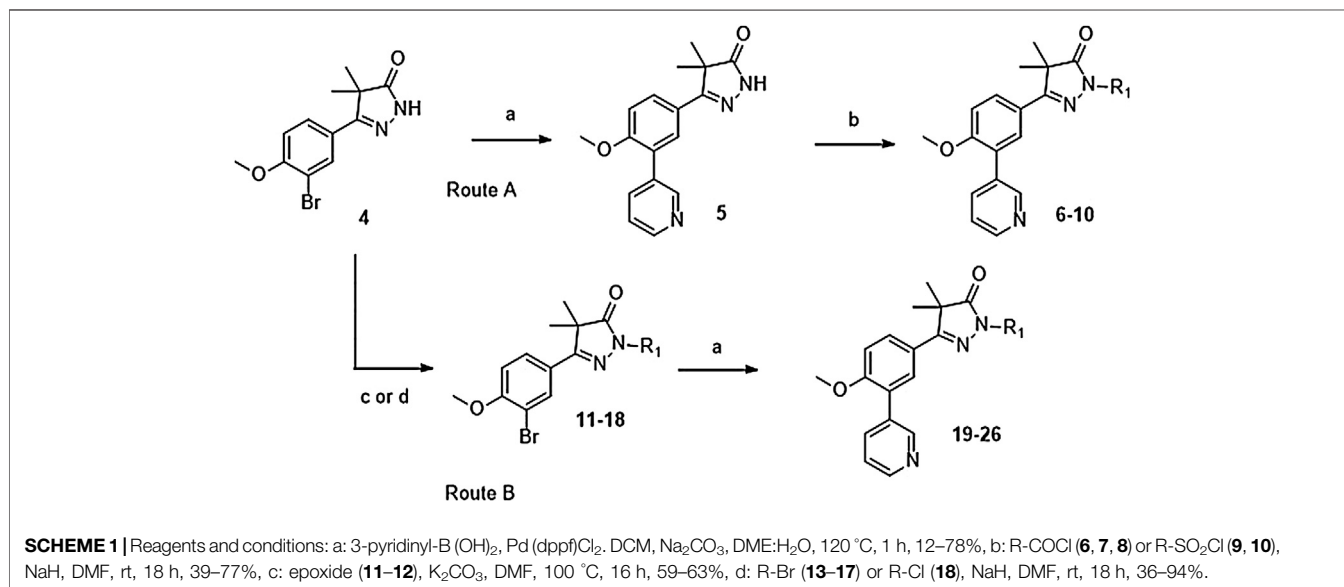
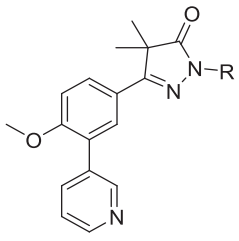
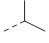
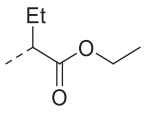
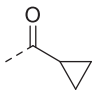
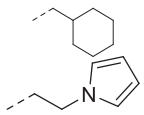
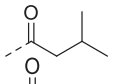
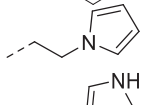
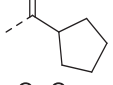
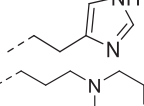
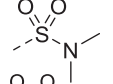
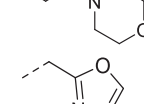
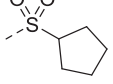
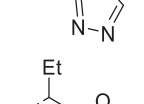
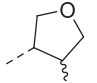
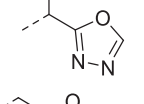
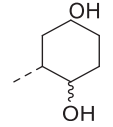
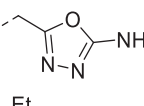
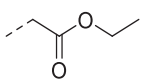
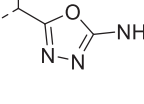


TABLE 1 | *In vitro* activity against intracellular amastigotes of *T. cruzi* (Tulahuen strain)^a and MRC-5 cells^a of phenyldihydropyrazolones with modifications directly on the pyrazolone nitrogen.


Cpd	R	<i>T. cruzi</i> (pIC ₅₀)	MRC-5 (pIC ₅₀)	SI ^b	cLogP	Cpd	R	<i>T. cruzi</i> (pIC ₅₀)	MRC-5 (pIC ₅₀)	SI ^b	cLogP
3		6.4	4.4	100	3.5	22		5.2	<4.2	>10	3.4
6		4.4	<4.2	>2	3.2	23		5.6	4.9	5	4.8
7		4.5	<4.2	>2	3.9	24		5.5	4.5	10	3.8
8		4.4	<4.2	>2	4.1	25		4.5	<4.2	>2	2.3
9		4.4	<4.2	>2	1.9	26		<4.2	<4.2	N.D.	2.5
10		5.0	4.4	4	3.6	33		5.1	<4.2	>8	1.5
19		4.4	<4.2	>2	1.9	34		5.2	<4.2	>10	2.5
20		5.1	<4.2	>8	3.4	35		4.2	4.2	0	1.3
21		5.2	<4.2	10	2.6	36		4.4	<4.2	2	2.4

^aAll reported values are measured as duplicates and had a standard deviation less than ± 0.2 .

^bSelectivity index was calculated as IC_{50} MRC-5 cells divided by IC_{50} *T. cruzi*.

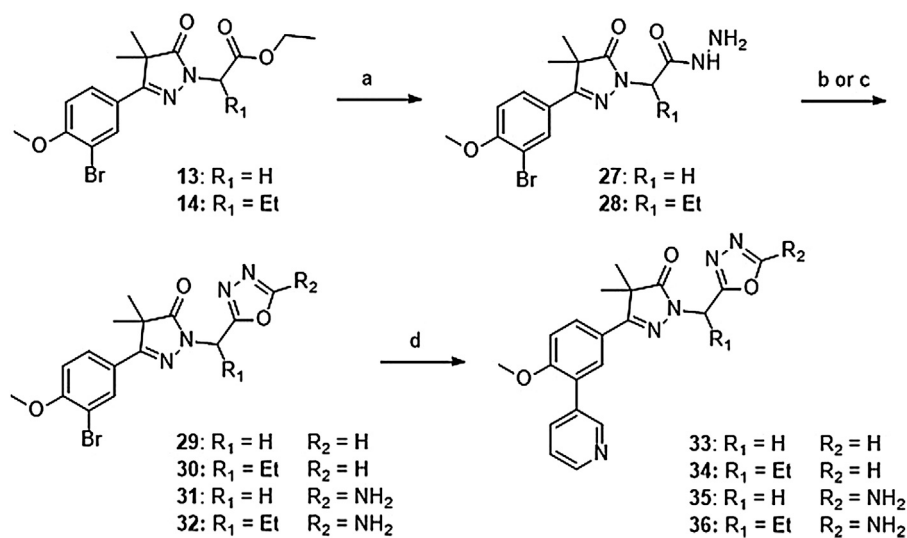
multiple times between hydrophobic and hydrophilic phases, as such an optimal cLogP is thought to be between 0 and 2 and the drug having no charges (Basore et al., 2015; Bennion et al., 2017).

Chemistry

Phenylpyrazolone analogues with a substituent directly on the pyrazolone nitrogen atom were synthesized using two different routes. The first route started with a Suzuki reaction to obtain dihydropyrazolone **5** (Route A, **Scheme 1**) which was then functionalized using sodium hydride and various acyl chlorides and sulfonylchlorides to obtain compounds **6–10** (**Table 1**). The second route (Route B) started with alkylation

of the dihydropyrazolone **4**, either using potassium carbonate to yield intermediates **11–12**, or using sodium hydride to generate intermediates **13–18**. These intermediates were then converted to the 3-pyridinyl derivatives *via* a Suzuki cross coupling, yielding final compounds **20–26** (**Scheme 1**, **Table 1**).

Introduction of methylene-oxadiazoles on the pyrazolone head group started with the previously synthesized ester analogues **13** and **14** (**Scheme 2**). Subsequent hydrazination yielded the corresponding hydrazides (**27** and **28**) which were ring-closed with either triethylorthoformate or cyanuric bromide to deliver the unsubstituted oxadiazoles (**29** and **31**) and the amine substituted oxadiazoles (**30** and **32**) respectively. These oxadiazoles were then converted to the



SCHEME 2 | Reagents and conditions: a: N₂H₄, EtOH, rt, 18 h, 90–94%, b: (EtO)₃CH, reflux, 18 h, 34–78% (**29–30**), c: BrCN, NaHCO₃, MeOH, H₂O, o. n., 22–46% (**31–32**), d: 3-pyridinyl-B(OH)₂, Pd(dppf)Cl₂, DCM, Na₂CO₃, DME:H₂O, 120 °C, 1 h 36–74%.

corresponding 3-pyridinyl analogues *via* a Suzuki cross-coupling to yield compounds **33–36**.

The synthesis of the piperidine substituted dihydropyrazolones started with keto-ester **37** (Scheme 3) which was prepared according to previously reported methodology (Sijm et al., 2019). This keto-ester was condensed with 4-hydrazinylpiperidine to yield piperidine substituted dihydropyrazolone **38**. The piperidine nitrogen atom was protected using boc-anhydride to give intermediate (**39**) which could be used in a Suzuki cross-coupling to install the 3-pyridine moiety. Subsequent deprotection of **40** with 4 M HCl in dioxane yielded the free amine building block (**41**) which was used to install the desired electrophiles (**42–83**, Tables 2,3) *via* various methodologies.

Pharmacology and Parasitology

All compounds were tested for their trypanocidal activity against intracellular forms of *T. cruzi* (Tulahuen CL2, β -galactosidase strain (drug sensitive strain (discrete typing units, DTU VI)) as well as for cytotoxicity on MRC-5_{SV2} cells (human lung fibroblasts). (Blaazer et al., 2014).

RESULTS AND DISCUSSION

In the previous work by Sijm *et al.*, the pyrazolone nitrogen was substituted with various (cyclo)-alkyl moieties resulting in the identification of NPD-0227 (**3**) as a potent (pIC₅₀ = 6.4) *T. cruzi* inhibitor with 100-fold selectivity over human MRC-5 cells (Table 1) (Sijm et al., 2019; Sijm et al., 2020). To further explore SAR and to investigate molecules with varying cLogPs, more polar and diverse substituents was explored.

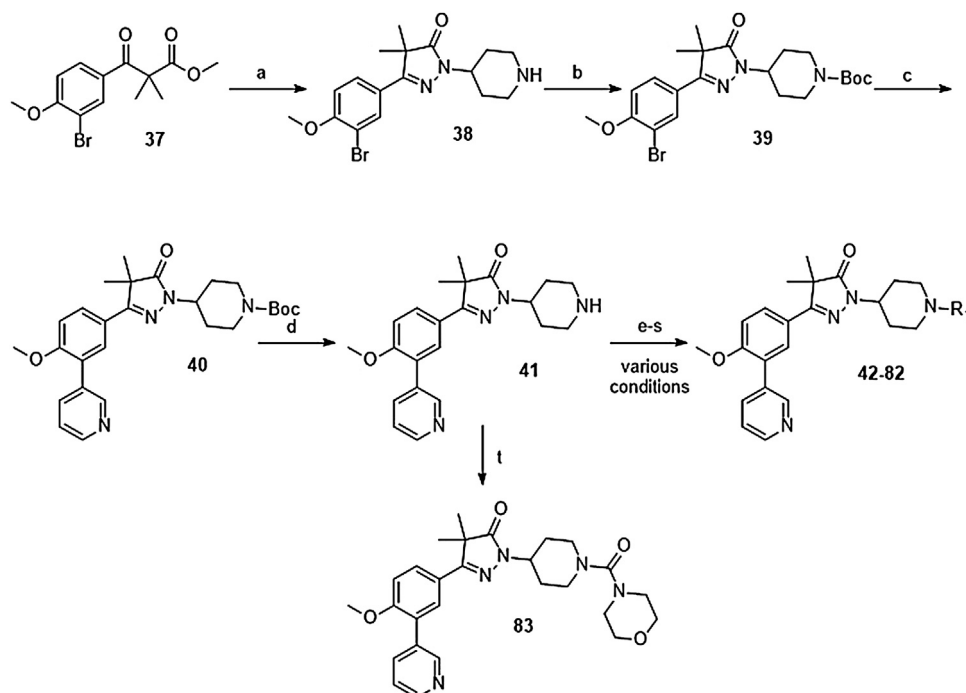
Introduction of a carbonyl-alkyl moieties directly onto the pyrazolone nitrogen (**6–8**, Table 1) resulted in weak inhibitors

with pIC₅₀'s around 4.5. Similarly, introduction of sulphonyl-alkyl moieties such as dimethylsulfonamide (**9**) or sulphonylcyclopentyl (**10**) did not lead to inhibitors with pIC₅₀ values above 5.0. Epoxides were used to introduce β -alcohols on the pyrazolone ring resulting in compounds **19** and **20**. These alcohols also showed a large decrease in activity compared to NPD-0227 (pIC₅₀ = 6.4) with pIC₅₀'s of 4.4 and 5.1, respectively. Similarly, the introduction of ethyl-esters (**21**, **22**) resulted in decreased potencies compared to NPD-0227 with both compounds showing pIC₅₀ values of only 5.2.

While the substituents with a polar moiety (**6–10**, **19–22**, Table 1) showed decreased activities, as expected, introduction of more apolar moieties such as methyl-cyclohexyl (**23**) and pyrazole (**24**) showed moderate activity with pIC₅₀ values of 5.5. Introduction of more polar substituents attached to an aliphatic linker, such as imidazole **25** and morpholine **26** with cLogPs around 2.3 resulted in lower potencies (pIC₅₀ < 4.6). While the introduction of various oxadiazoles (**33–36**) on this position yielded compounds with a more desirable cLogP's, this did not lead to very active compounds, with 1-propan-oxazole (**34**) showed the highest potency (pIC₅₀ = 5.2). As activities were generally close to the lower detection limit of the assay, selectivity indexes were quite low or defined as “bigger than”.

The initial attempts to introduce polar functional groups such as carbonyls, sulphonyls and alcohols close to the pyrazolone ring had a negative effect on their potency. One of the most potent compounds so far was methylcyclohexyl **23**, a bulky and apolar substituent. It was thought that introduction of a piperidine would introduce a similar sized moiety which would improve options to introduce polarity as a new handle to further modify.

This piperidine linker was first investigated by forming amides with corresponding acid chlorides or carboxylic acids, which led to analogues **42–47** (Table 2). These groups introduced some polarity but these modifications did not lead to potent ligands



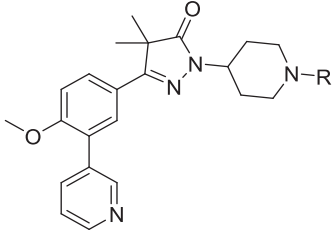
SCHEME 3 | Reagents and conditions: a: 4-hydrazinylpiperidine.2HCl, MeOH, H₂O, reflux, 3 days, 80%, b: Boc₂O, TEA, DCM, rt, 4 h, 89%, c: 3-pyridinyl-B(OH)₂, Pd(dppf)Cl₂, DCM, Na₂CO₃, DME:H₂O, 120 °C, 1 h, 86%, d: 4 M HCl in dioxane, rt, 18 h, 84%, e: R-COCl (**42, 43**), R-SO₂Cl (**48**), NaH, DMF, rt, 2 h, 38–42%, f: EDCl, HOBT, RCOOH (**44, 46**), DIPEA, DCM, 18–30 h, 23–31%, g: oxazole-5-carboxylic acid (**45**), T3P, DIPEA, EtOAc, 50 °C, 70 h, 7%, h: R-COCl (**47**) or R-SO₂Cl (**49–54**) or OCN-R (**55, 57–59, 61**) or Cl(CO)NR₁R₂ (**56, 60**), TEA, DCM, rt, 2–42 h, 13–79%, i: epoxide (**62–66**), DMAP, i-PrOH, 50–100 °C, 2–120 h, 4–30%, j: formic acid (**67**), formaldehyde, 18 h, rt, 15%, k: R-CO-R (**68–69, 71, 74**), NaBH(OAc)₃, AcOH, DCE, 70 °C, 18–72 h, 10–53%, l: R-Br (**70**), K₂CO₃, DMF, rt, 48 h, 10%, m: methylacrylate (**72**), DBN, ACN, 90h, rt, 45%, n: ClCH₂CO-R (**73**), K₂CO₃, ACN, 24 h, rt, 39%, o: HCO-R (**74–78**), NaBH(OAc)₃, AcOH, DCE, 22–72 h, 5–48%, q: Ar-Br (**79–80**), Pd₂(dba)₃, BINAP, NaOtBu, 80 °C, 7 days, 11–19%, r: Cl-Ar (**81**), Cs₂CO₃, DMF, 90 °C, 4 h, 24%, s: F-Ar (**82**), DMSO, K₂CO₃, 110 °C, 6 days, 16% t: i: (**83**) NaHCO₃, 4-NO₂Ph-chloroformate, dioxane, rt, 22 h, ii: K₂CO₃, morpholine, DMF, rt, 4 days.

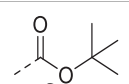
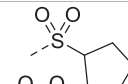
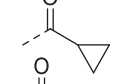
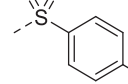
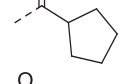
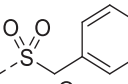
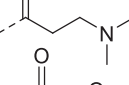
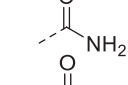
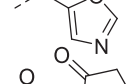
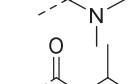
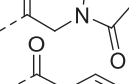
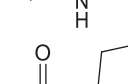
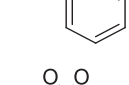
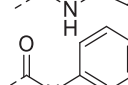
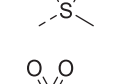
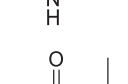
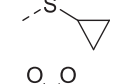
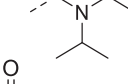
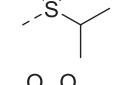
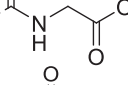
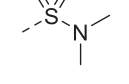
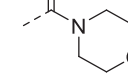
(pIC₅₀ < 5.3). Introducing sulphonamides instead of regular amides gave similar results as the majority showed moderately low activity (**48–54**). Alkyl-sulphonamides with a cyclopropyl (**49**), isopropyl (**50**), dimethylamino (**51**) and cyclopentyl (**52**) all showed pIC₅₀'s around 5.1, while the smaller methyl substituted sulphonamide (**48**) had a slightly lower activity (pIC₅₀ = 4.5). Introduction of an aromatic ring on to the sulphonamide did not have a positive effect. Tosylate **53** (cLogP = 4.4) was inactive with a pIC₅₀ below 4.2. Introduction of an extra carbon between the sulphonamide and the benzene ring was successful as methylbenzyl **54** (cLogP = 3.8) showed a similar potency as NPd-0227 (**3**, Table 1) with a pIC₅₀ value of 6.2 and >100-fold selectivity over human MRC-5.

The boc-protected analogue **40** (cLogP = 3.6; pIC₅₀ = 5.9, Table 2) which was obtained during the synthesis of the free-amine building block showed that relatively large substituents are allowed on the piperidine linker, which was confirmed by sulphonamide **54**. The preference for larger, bulky substituents is also apparent with the urea linked analogues (**55–59**). While the carbamide is inactive (**55**, cLogP = 1.6; pIC₅₀ = <4.2), introduction of larger apolar groups increased activity (**57–59**), with the most potent compound being the 4-fluorophenyl **59** (pIC₅₀ = 5.9; cLogP = 4.0, 25-fold selectivity). The even more bulky disopropyl analogue (**60**),

however, was totally inactive (pIC₅₀ < 4.2). Introduction of more polar substituents attached to the urea linker did not improve activity with pIC₅₀ values of <4.2 for ethylacetate derivative **61** (cLogP = 1.8) and 4.9 for the morpholine analogue (**83**, cLogP = 1.8). Two types of epoxides were used to introduce β-alcohols. While the aliphatic analogues **62–64** (Table 3) showed low potencies (pIC₅₀ < 4.6), the aromatic derivatives (**65–66**) showed micromolar activities with pIC₅₀ values of 5.6 and 5.7. Selectivity of the unsubstituted phenyl ring (**65**) was however a lot better than the 4-fluorophenyl (**66**).

As shown in Table 1 and in previous work, aliphatic substituents on the dihydropyrazolone nitrogen led to the most potent compounds (Sijm et al., 2019). Introduction of aliphatic substituents on the piperidine nitrogen resulted in poor potencies, possibly caused by the introduction of a tertiary amine which can be protonated, as charged compounds are less likely to cross the cell membrane. The unsubstituted piperidine (**41**, cLogP = 2.3, Table 3) is totally inactive (pIC₅₀ < 4.2) and the alkylated analogues (**67–73**) are not very active inhibitors (pIC₅₀ < 5.0). Analogues with an aromatic ring showed higher activities: the 2-furanylmethyl (**74**, cLogP = 3.5) and the 3-pyridinylmethyl (**77**, cLogP = 4.4) showed pIC₅₀ values of 5.0 and 5.3, respectively. The benzyl substituted

TABLE 2 | *In vitro* activity against intracellular amastigotes of *T. cruzi* (Tulahuen strain)^a and MRC-5 cells^a of phenyldihydropyrazolones with a piperidine linker.


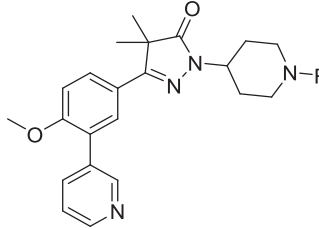
Cpd	R	<i>T. cruzi</i> (pIC ₅₀)	MRC-5 (pIC ₅₀)	SI ^b	cLogP	Cpd	R	<i>T. cruzi</i> (pIC ₅₀)	MRC-5 (pIC ₅₀)	SI ^b	cLogP
40		5.9	<4.2	>50	3.6	52		5.2	4.5	5	3.1
42		4.4	<4.2	>2	2.7	53		<4.2	<4.2	N.D.	4.4
43		5.2	4.5	5	3.6	54		6.2	<4.2	>100	3.8
44		4.5	<4.2	>2	2.1	55		<4.2	<4.2	N.D.	1.6
45		4.6	<4.2	>3	1.6	56		4.5	<4.2	>2	2.0
46		<4.2	<4.2	N.D.	0.9	57		4.9	<4.2	>5	2.6
47		<4.2	<4.2	N.D.	3.8	58		5.5	4.5	10	3.2
48		4.5	<4.2	>2	1.4	59		5.9	4.5	25	4.0
49		5.0	<4.2	>6	2.2	60		<4.2	<4.2	N.D.	3.6
50		5.1	<4.2	>8	2.5	61		<4.2	<4.2	N.D.	1.8
51		5.1	<4.2	>8	1.4	83		4.9	<4.2	>5	1.8

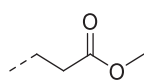
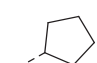
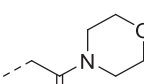
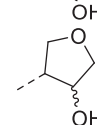
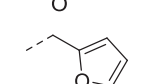
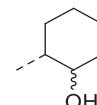
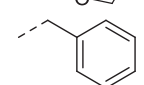
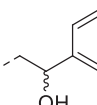
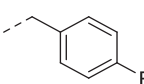
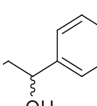
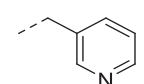
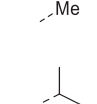
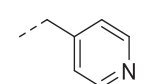

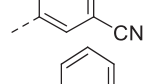

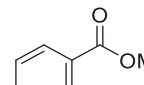
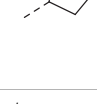
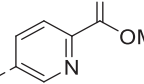
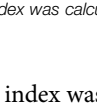

^aAll reported values are measured as duplicates and had a standard deviation less than ± 0.2 .

^bSelectivity index was calculated as IC₅₀ MRC-5 cells divided by IC₅₀ *T. cruzi*.

piperidine **75** and the 4-pyridinemethyl **78** both showed pIC₅₀ values around 5.6, while 4-fluorobenzyl **76** (cLogP = 4.6) showed sub-micromolar potency with a pIC₅₀ of 6.1. Selectivity indexes of these compounds were moderate to poor, with the best compound, 4-pyridinemethyl **78** showing 16-fold selectivity toward *T. cruzi* over MRC-5 cells.

The final set of substituents on the piperidine linker were aromatic rings (Table 3, **79–82**). This sub-series showed moderate activities with the 3-cyanophenyl (**79**), 4-methylbenzoate (**81**) and methyl-5-picolinate (**82**) all having low micromolar activities (pIC₅₀ = 5.7). The 3-pyridinyl analogue (**80**) was less active with a pIC₅₀ of 5.2. Best

TABLE 3 | *In vitro* activity against intracellular amastigotes of *T. cruzi* (Tulahuen strain)^a and MRC-5 cells^a toxicity by phenylidihydropyrazolones with a piperidine linker.


Cpd	R	<i>T. cruzi</i> (pIC ₅₀)	MRC-5 (pIC ₅₀)	SI ^b	cLogP	Cpd	R	<i>T. cruzi</i> (pIC ₅₀)	MRC-5 (pIC ₅₀)	SI ^b	cLogP
41	H	<4.2	<4.2	N.D.	2.3	72		<4.2	<4.2	N.D.	2.6
62		4.5	4.5	1	3.0	73		4.4	<4.2	>2	1.6
63		<4.2	<4.2	N.D.	1.9	74		5.0	4.6	3	3.5
64		4.5	4.6	<1	3.4	75		5.6	4.6	10	4.4
65		5.6	<4.2	>25	3.8	76		6.1	5.1	10	4.6
66		5.7	5.2	3	3.9	77		5.3	4.5	6	3.2
67		4.4	<4.2	>2	2.7	78		5.7	4.5	16	3.2
68		4.5	<4.2	>2	3.5	79		5.7	<4.2	>32	4.4
69		4.9	4.5	3	3.6	80		5.2	4.5	5	3.4
70		4.8	4.5	2	3.5	81		5.7	5.0	5	4.6
71		4.6	4.5	1	4.1	82		5.7	<4.2	>32	4.0

^aAll reported values are measured as duplicates and had a standard deviation less than ± 0.2 .

^bSelectivity index was calculated as IC₅₀ MRC-5 cells divided by IC₅₀ *T. cruzi*.

selectivity index was observed for 3-cyanophenyl **79** and methyl-5-picolinate **82**, which both had over 32-fold selectivity.

Overall, the introduction of polar moieties on the phenylidihydropyrazolones generally led to low activities against *T. cruzi*.

Especially the introduction of a polar moiety directly next to the pyrazolone nitrogen such as all carbonyl, sulphonyl and β -alcohol linked moieties (**6–10**, **19**, **20**) resulted in analogues with low potencies. Introduction of aliphatic substituents or aromatic

moieties resulted in interesting new anti-*T. cruzi* inhibitors with the best compounds **54** and **76** reaching sub micromolar potency. Installing a piperidine linker allowed for the introduction of a variety of substituents and it became apparent that aromatic moieties, either directly, with a methylene bridge or with a 2-atom linker performed best, showing pIC₅₀'s around 6.0.

CONCLUSION

Our study results in valuable SAR data that has been obtained by introducing a variety of substituents on the dihydropyrazolone nitrogen atom. While decorating this position is synthetically very efficient and a wide variety of chemical functionalities are allowed, our studies did not lead to compounds that have a better activity than NPD-0227. Especially the piperidine linker opens a whole new range of options to introduce substituents and analogues reached low micromolar inhibitory activities against *T. cruzi*. The most active compounds were obtained if the piperidine is substituted with apolar moieties such as aryl or benzyl rings. Introduction of more polar substituents, such as imidazole **25** (cLogP = 2.3), succinimide **46** (cLogP = 0.9) and morpholine **73** (cLogP = 1.6) generally lead to compounds with high micromolar activities. The structural moiety performing best is a 2-atom linker followed by an aromatic moiety, of which sulphonamide **54** (cLogP = 3.8), urea **59** (cLogP = 4.0) and β -alcohols **65** and **66** (cLogP = 3.8/3.9) performed best. These molecules all have activities around 6.0 (pIC₅₀) and especially sulphonamide **54** is promising with a pIC₅₀ of 6.2 and >100-fold selectivity over MRC-5 cells. Also other aromatic substituents performed well, such as 4-fluorobenzyl (**76**), 3-cyanophenyl (**79**) and 5-methylnicotinate (**82**) show promising activities around 6.0, with **79** and **82** showing best selectivities (>32-fold) toward *T. cruzi*. While these results of this study are important in the design of novel 'drug leads' for Chagas disease, the original goal, of identifying high potency molecules with a lower cLogP did not succeed. Most potent compounds with a cLogP below 2.0 were oxadiazole **33** and sulfamide **51**, which both showed a pIC₅₀ of 5.1.

Experimental Section Biology

Trypanosoma cruzi *in vitro* assay. Bloodstream trypomastigotes of the Y strain of *T. cruzi* were obtained by cardiac puncture of infected Swiss Webster mice on the parasitaemia peak (Meirelles et al., 1986; Batista et al., 2010). For the standard *in vitro* susceptibility assay on intracellular amastigotes, *T. cruzi* Tulahuen CL2, β -galactosidase strain (nifurtimox-sensitive) was used. The strain is maintained on MRC-5_{SV2} (human lung fibroblast) cells in MEM medium, supplemented with 200 mM L-glutamine, 16.5 mM NaHCO₃ and 5% inactivated fetal calf serum (FCSi). All cultures and assays were conducted at 37°C under an atmosphere of 5% CO₂. Benznidazole was included in the assays as a positive control.

MRC-5 cytotoxicity in vitro assay. MRC-5_{SV2} cells, originally from a human diploid lung cell line, were cultivated in MEM supplemented with L-glutamine (20 mM), 16.5 mM sodium hydrogen carbonate and 5% FCSi. For the assay, 10⁴ cells/well

were seeded onto the test plates containing the pre-diluted sample and incubated at 37°C and 5% CO₂ for 72 h. Cell viability was assessed fluorometrically 4 h after addition of resazurin (excitation 550 nm, emission 590 nm). The results are expressed as percentage reduction in cell viability compared to untreated controls. Tamoxifen was included in the assays as a positive control.

The use of laboratory rodents was carried out in strict accordance to all mandatory guidelines (EU directives, including the Revised Directive 2010/63/EU on the Protection of Animals used for Scientific Purposes that came into force on January 1, 2013, and the Declaration of Helsinki in its latest version).

Experimental Section Chemistry

Chemicals and reagents were obtained from commercial suppliers and were used without further purification. Anhydrous DMF, THF, and DCM were obtained by passing them through an activated alumina column prior to use. Microwave reactions were executed using a Biotage[®] Initiator microwave system. ¹H NMR spectra were recorded on a Bruker Avance 250 (250 MHz), Bruker Avance 400 (400 MHz), Bruker Avance 500 (500 MHz) or Bruker 600 Avance (600 MHz) spectrometer. Data are reported as follows: chemical shift, integration, multiplicity (s = singlet, d = doublet, dd = double doublet, t = triplet, dt = double triplet, q = quartet, p = pentet, h = heptet, bs = broad singlet, m = multiplet), and coupling constants (Hz). Chemical shifts are reported in ppm with the natural abundance of deuterium in the solvent as the internal reference [CDCl₃: δ 7.26, (CD₃)₂SO: δ 2.50]. ¹³C NMR spectra were recorded on a Bruker Avance 500 (126 MHz) or Bruker Avance 600 (150 MHz). Chemical shifts are reported in ppm with the solvent resonance resulting from incomplete deuteration as the internal reference [CDCl₃: δ 77.16 or (CD₃)₂SO: δ 39.52]. Systematic names for molecules according to IUPAC rules were generated using the Chemdraw AutoName program. LC-MS data was gathered using a Shimadzu HPLC/MS workstation with a LC-20AD pump system, SPD-M20A diode array detection, and a LCMS-2010 EV mass spectrometer. The column used is an Xbridge C18 5 μ m column (100 mm \times 4.6 mm). Solvents used were the following: solvent B = ACN, 0.1% formic Acid; solvent A = water, 0.1% formic acid. The analysis was conducted using a flow rate of 1.0 ml/min, start 5% B, linear gradient to 90% B in 4.5 min, then 1.5 min at 90% B, linear gradient to 5% B in 0.5 min and then 1.5 min at 5% B, total run time of 8 min. All reported compounds have purities >95%, measured at 254 nm, unless otherwise mentioned. All HRMS spectra were recorded on a Bruker micrOTOF mass spectrometer using ESI in positive-ion mode. In case of bromine containing molecules, the lowest peak of ⁷⁹Br was reported. Column purifications were either carried out automatically using Biotage equipment or manually, using 60–200 mesh silica. TLC analyses were performed with Merck F254 alumina silica plates using UV visualization. All reactions were done under N₂ atmosphere, unless

specifically mentioned. The cLogPs were calculated using CDD vault, CDD vault uses the ionic logP algorithm.

Experimental Data

Compound **5**, **6**, **15**, **23**, **27**, **29**, **33**, **38–42** and **83** are described below, other compounds can be found in the supporting information.

3-(4-Methoxy-3-(pyridin-3-yl)phenyl)-4,4-dimethyl-1H-pyrazol-5(4H)-one (**5**)

Pyrazolone **4** (1.0 g, 3.4 mmol) and pyridin-3-ylboronic acid (0.62 g, 5.1 mmol) were charged to a microwave tube after which DME (12 ml) and 1 M Na₂CO₃ (6.7 ml, 6.7 mmol) were added. The mixture was degassed with N₂ for 5 m after which Pd (dppf)Cl₂ (0.28 g, 34 mmol) was added. The reaction was heated at 120°C for 1 h in the microwave. The reaction mixture was diluted with EtOAc (30 ml) and filtered over Celite. The residue was washed with saturated NaHCO₃ (2 ml × 30 ml) and brine (1 ml × 30 ml). The organic phase was dried over Na₂SO₄, filtered and concentrated *in vacuo*. The remaining crude was purified over SiO₂ using a gradient of 50% EtOAc in heptane toward 5% MeOH in EtOAc to yield 700 mg (2.4 mmol, 70%) of the title compound as a white solid. ¹H NMR (500 MHz, CDCl₃) δ 11.50 (s, 1H), 8.69 (s, 1H), 8.55 (d, *J* = 3.8 Hz, 1H), 7.91 (apparent dt, *J* = 7.9, 1.9 Hz, 1H), 7.84 (dd, *J* = 8.7, 2.3 Hz, 1H), 7.73 (d, *J* = 2.3 Hz, 1H), 7.46 (dd, *J* = 7.9, 4.8 Hz, 1H), 7.22 (d, *J* = 8.8 Hz, 1H), 3.83 (s, 3H), 1.37 (s, 6H). ¹³C NMR (126 MHz, CDCl₃) δ 181.1, 161.6, 157.7, 150.0, 148.6, 137.1, 133.7, 128.1, 128.0, 127.4, 124.4, 123.8, 112.4, 56.3, 46.9, 22.5. LC-MS (ESI) *m/z* found: 296 (M + H)⁺; retention time: 2.67 min. HRMS-ESI (M + H)⁺ calculated for C₁₇H₁₈N₃O₂: 296.1394, found: 296.1391.

1-(cyclopropanecarbonyl)-3-(4-Methoxy-3-(Pyridin-3-Yl)phenyl)-4,4-Dimethyl-1h-Pyrazol-5(4H)-One (**6**)

Pyrazolone **5** (50 mg, 0.17 mmol) was dissolved in DMF (2 ml) and sodium hydride (60% in mineral oil) (10 mg, 0.25 mmol) was added. After stirring for 30 min cyclopropanecarbonyl chloride (20 mg, 0.19 mmol) was added and the mixture was stirred at rt for 18 h after which the reaction was quenched with water (25 ml) and extracted with EtOAc (25 ml). The organic layer was washed with sat. aq. NaHCO₃ (2 ml × 20 ml), brine (20 ml) and dried over MgSO₄ after which volatiles were evaporated yielding 24 mg (0.07 mmol, 39%) of the title compound as a white solid. ¹H NMR (500 MHz, CDCl₃) δ 8.76 (d, *J* = 2.0 Hz, 1H), 8.60 (dd, *J* = 4.8, 1.7 Hz, 1H), 7.95–7.84 (m, 3H), 7.38 (dd, *J* = 7.8, 4.8 Hz, 1H), 7.09–7.03 (m, 1H), 3.89 (s, 3H), 3.05–2.97 (m, 1H), 1.61 (s, 6H), 1.32–1.25 (m, 2H), 1.11–1.02 (m, 2H). ¹³C NMR (126 MHz, CDCl₃) δ 178.0, 171.9, 162.3, 158.7, 150.0, 148.3, 137.1, 133.3, 129.5, 128.7, 127.8, 123.1, 122.9, 111.2, 55.8, 49.9, 23.2, 13.5, 11.3. LC-MS (ESI) *m/z* found: 364 (M + H)⁺; retention time: 3.43 min. HRMS-ESI (M + H)⁺ calculated for C₂₁H₂₂N₃O₃: 364.1656, found: 364.1653.

Ethyl 2-(3-(3-bromo-4-methoxyphenyl)-4,4-dimethyl-5-oxo-4,5-dihydro-1H-pyrazol-1-yl)acetate (**13**)

Pyrazolone **4** (5.0 g, 16.8 mmol) was dissolved in DMF (35 ml) and sodium hydride (60% in mineral oil) (0.49 g, 20.2 mmol) was added. After stirring for 30 min ethyl 2-bromoacetate (2.23 ml,

20.2 mmol) was added and the mixture was heated to 50°C for 3 h after which the reaction was quenched with water (250 ml). Solids were filtered off and dried *in vacuo*, yielding 5.6 g (14.6 mmol, 87%) of the title compound as a white solid. ¹H NMR (500 MHz, CDCl₃) δ 8.05 (d, *J* = 2.2 Hz, 1H), 7.70 (dd, *J* = 8.6, 2.2 Hz, 1H), 6.93 (d, *J* = 8.7 Hz, 1H), 4.55 (s, 2H), 4.23 (q, *J* = 7.1 Hz, 2H), 3.95 (s, 3H), 1.53 (s, 6H), 1.29 (t, *J* = 7.1 Hz, 3H). ¹³C NMR (126 MHz, CDCl₃) δ 179.1, 167.8, 160.9, 157.2, 131.4, 126.7, 124.6, 112.3, 111.5, 61.7, 56.4, 48.1, 45.8, 22.5, 14.1. LC-MS (ESI) *m/z* found: 383 (M + H)⁺; retention time: 4.75 min. HRMS-ESI (M + H)⁺ calculated for C₁₆H₂₀BrN₂O₄: 383.0601, found: 383.0588.

3-(3-Bromo-4-methoxyphenyl)-1-(cyclohexylmethyl)-4,4-dimethyl-1H-pyrazol-5(4H)-one (**15**)

Pyrazolone **4** (100 mg, 0.30 mmol) was dissolved in DMF (3 ml) and sodium hydride (60% in mineral oil) (15 mg, 0.38 mmol) was added. After stirring for 30 min (bromomethyl)cyclohexane (63 mg, 0.67 mmol) was added and the mixture was stirred at rt for 18 h after which the reaction was quenched with water (25 ml) and extracted with EtOAc (25 ml). The organic layer was washed with brine (2 ml × 20 ml) and dried over MgSO₄ after which volatiles were evaporated yielding 105 mg (0.27 mmol, 91%) of the title compound as a transparent oil. ¹H NMR (500 MHz, CDCl₃) δ 8.03 (d, *J* = 2.2 Hz, 1H), 7.66 (dd, *J* = 8.6, 2.2 Hz, 1H), 6.90 (d, *J* = 8.7 Hz, 1H), 3.92 (s, 3H), 3.56 (d, *J* = 7.2 Hz, 2H), 1.89–1.80 (m, 1H), 1.74–1.68 (m, 2H), 1.67–1.61 (m, 3H), 1.45 (s, 6H), 1.28–1.13 (m, 5H), 1.08–0.89 (m, 2H). ¹³C NMR (126 MHz, CDCl₃) δ 178.6, 160.1, 156.9, 131.2, 126.5, 125.0, 112.3, 111.5, 56.4, 50.3, 48.3, 36.9, 30.5, 26.4, 25.7, 22.8. LC-MS (ESI) *m/z* found: 393 (M + H)⁺; retention time: 6.05 min. HRMS-ESI (M + H)⁺ calculated for C₁₉H₂₆BrN₂O₂: 393.1172, found: 393.1156.

1-(cyclohexylmethyl)-3-(4-Methoxy-3-(Pyridin-3-Yl)phenyl)-4,4-Dimethyl-1h-Pyrazol-5(4H)-One (**23**)

Pyrazolone **15** (100 mg, 0.16 mmol) and pyridin-3-ylboronic acid (47 mg, 0.38 mmol) were charged to a microwave tube after which DME (3 ml) and 1 M Na₂CO₃ (0.8 ml, 0.8 mmol) were added. The mixture was degassed with N₂ for 5 m after which Pd (dppf) Cl₂ (21 mg, 25 μmol) was added. The reaction was heated at 120°C for 1 h in the microwave. The reaction mixture was diluted with EtOAc (30 ml) and filtered over Celite. The residue was washed with saturated NaHCO₃ (2 ml × 30 ml) and brine (1 ml × 30 ml). The organic phase was dried over Na₂SO₄, filtered and concentrated *in vacuo*. The remaining crude was purified over SiO₂ using a gradient of 50% EtOAc in heptane toward 100% EtOAc to yield 64 mg (0.16 mmol, 64%) of the title compound as a white solid. ¹H NMR (500 MHz, CDCl₃) δ 8.78 (d, *J* = 2.1 Hz, 1H), 8.59 (d, *J* = 4.8 Hz, 1H), 7.88 (apparent dt, *J* = 7.8, 1.9 Hz, 1H), 7.82 (d, *J* = 2.2 Hz, 1H), 7.77 (dd, *J* = 8.6, 2.2 Hz, 1H), 7.37 (dd, *J* = 7.9, 4.9 Hz, 1H), 7.03 (d, *J* = 8.6 Hz, 1H), 3.87 (s, 3H), 3.58 (d, *J* = 7.2 Hz, 2H), 2.05–1.79 (m, 2H), 1.76–1.60 (m, 5H), 1.50 (s, 6H), 1.29–1.10 (m, 3H), 1.06–0.95 (m, 2H). ¹³C NMR (126 MHz, CDCl₃) δ 178.7, 161.0, 157.8, 150.1, 148.2, 137.0, 133.6, 128.7, 127.6, 127.5, 124.2, 123.1, 111.1, 55.8, 50.3, 48.4, 36.9, 30.5, 26.4, 25.7, 22.9. LC-MS (ESI) *m/z* found: 392 (M + H)⁺; retention time:

4.54 min. HRMS-ESI (M + H)⁺ calculated for C₂₄H₃₀N₃O₂: 392.2333, found: 392.2319.

2-(3-(3-bromo-4-methoxyphenyl)-4,4-dimethyl-5-oxo-4,5-dihydro-1H-pyrazol-1-yl)acetohydrazide (27)

Ester **13** (1.5 g, 3.91 mmol) was refluxed in hydrazine monohydrate (1.89 ml, 39.1 mmol) and ethanol (25 ml) for 18 h. After that the mixture was allowed to cool down, the mixture was concentrated and 20 ml of water was added. The solids were filtered off and dried *in vacuo* yielding 1.36 g (3.7 mmol, 94%) of the title compound as a white solid. ¹H NMR (500 MHz, DMSO-*d*₆) δ 9.29 (s, 1H), 7.96 (s, 1H), 7.79 (d, *J* = 8.6 Hz, 1H), 7.17 (d, *J* = 8.6 Hz, 1H), 4.29 (d, *J* = 13.2 Hz, 4H), 3.90 (s, 3H), 1.39 (s, 6H). ¹³C NMR (126 MHz, DMSO-*d*₆) δ 178.9, 166.4, 160.0, 157.0, 130.5, 127.6, 124.6, 113.1, 111.8, 56.9, 47.7, 45.9, 22.4. LC-MS (ESI) *m/z* found: 369 (M + H)⁺; retention time: 3.59 min.

1-((1,3,4-Oxadiazol-2-yl)methyl)-3-(3-bromo-4-methoxyphenyl)-4,4-dimethyl-1H-pyrazol-5(4H)-one (29)

Hydrazide **27** (200 mg, 0.54 mmol) was stirred in triethylorthoformate (0.9 ml, 5.4 mmol) and PTSA (10.30 mg, 0.054 mmol) was added. The mixture was heated at 80°C for 18 h after which the volatiles were evaporated and the resulting crude was purified over SiO₂ using a gradient of 20% EtOAc in heptane toward 80% EtOAc in heptane. This yielded 70 mg (0.19 mmol, 34%) of the title compound as a white solid. ¹H NMR (500 MHz, CDCl₃) δ 8.42 (s, 1H), 7.99 (d, *J* = 2.2 Hz, 1H), 7.66 (dd, *J* = 8.7, 2.2 Hz, 1H), 6.90 (d, *J* = 8.7 Hz, 1H), 5.22 (s, 2H), 3.92 (s, 3H), 1.52 (s, 6H). ¹³C NMR (126 MHz, CDCl₃) δ 178.5, 161.9, 161.6, 157.4, 153.6, 131.4, 126.9, 124.2, 112.3, 111.6, 56.4, 48.1, 39.0, 22.6. LC-MS (ESI) *m/z* found: 397 (M + H)⁺; retention time: 4.27 min. HRMS-ESI (M + H)⁺ calculated for C₁₅H₁₆BrN₄O₃: 379.0400, found: 379.0391.

1-((1,3,4-Oxadiazol-2-yl)methyl)-3-(4-methoxy-3-(pyridin-3-yl)phenyl)-4,4-dimethyl-1H-pyrazol-5(4H)-one (33)

Pyrazolone **29** (50 mg, 0.13 mmol) and pyridin-3-ylboronic acid (24 mg, 0.38 mmol) were charged to a microwave tube after which DME (3 ml) and 1 M Na₂CO₃ (0.5 ml, 0.5 mmol) were added. The mixture was degassed with N₂ for 5 m after which Pd (dppf) Cl₂ (11 mg, 13 μmol) was added. The reaction was heated at 120°C for 1 h in the microwave. The reaction mixture was diluted with EtOAc (30 ml) and filtered over Celite. The residue was washed with saturated NaHCO₃ (2 ml × 30 ml) and brine (1 ml × 30 ml). The organic phase was dried over Na₂SO₄, filtered and concentrated *in vacuo*. The remaining crude was purified over SiO₂ using a gradient of 50% EtOAc in heptane toward 100% EtOAc to yield 36 mg (0.10 mmol, 72%) of the title compound as a white solid. ¹H NMR (500 MHz, CDCl₃) δ 8.79 (s, 1H), 8.61 (s, 1H), 8.41 (s, 1H), 7.95–7.83 (m, 1H), 7.83–7.73 (m, 2H), 7.41 (s, 1H), 7.03 (d, *J* = 8.4 Hz, 1H), 5.23 (s, 2H), 3.87 (s, 3H), 1.56 (s, 6H). ¹³C NMR (126 MHz, CDCl₃) δ 178.6, 162.4, 162.0, 158.2, 153.6, 149.5, 147.6, 137.5, 133.9, 128.9, 128.0, 127.4, 123.4, 111.2,

55.9, 48.2, 39.0, 22.8. LC-MS (ESI) *m/z* found: 378 (M + H)⁺; retention time: 2.93 min. HRMS-ESI (M + H)⁺ calculated for C₂₀H₂₀N₅O₃: 378.1562, found: 378.1562.

3-(3-Bromo-4-methoxyphenyl)-4,4-dimethyl-1-(piperidin-4-yl)-1H-pyrazol-5(4H)-one (38)

Keto-ester **37** (32 g, 102 mmol) was dissolved in methanol (200 ml) and stirred. To this solution 4-hydrazinylpiperidine dihydrochloride (76 g, 406 mmol) dissolved in Water (80 ml) was added. The mixture was refluxed for 72 h after which 150 ml water was added and MeOH was removed *in vacuo*. To the remaining solution 10 M NaOH was added slowly until the pH was ~13. Solids were collected and washed with water (20 ml) to yield 31 g (82 mmol, 80%) of the title compound. ¹H NMR (500 MHz, CDCl₃) δ 8.00 (d, *J* = 2.2 Hz, 1H), 7.78 (dd, *J* = 8.6, 2.2 Hz, 1H), 7.16 (d, *J* = 8.8 Hz, 1H), 4.06–3.94 (m, 1H), 3.90 (s, 3H), 3.04–2.93 (m, 2H), 2.53–2.51 (m, 2H), 1.84–1.75 (m, 2H), 1.66–1.56 (m, 2H), 1.35 (s, 6H). ¹³C NMR (126 MHz, CDCl₃) δ 177.5, 159.7, 156.9, 130.4, 127.4, 124.8, 113.1, 111.9, 56.9, 51.5, 48.4, 45.6, 31.7, 22.4. LC-MS (ESI) *m/z* found: 380 (M + H)⁺; retention time: 3.19 min. HRMS-ESI (M + H)⁺ calculated for C₁₇H₂₃BrN₃O₂: 380.0968, found: 380.0968.

Tert-butyl 4-(3-(3-bromo-4-methoxyphenyl)-4,4-dimethyl-5-oxo-4,5-dihydro-1H-pyrazol-1-yl)piperidine-1-carboxylate (39)

Piperidine **38** (25 g, 65.7 mmol) was added to a round-bottom flask after which DCM (500 ml) was added, followed by di-tert-butyl dicarbonate (15.6 ml, 67.1 mmol) and triethylamine (9.4 ml, 67.1 mmol). The reaction mixture was extracted with water (2 ml × 400 ml) and brine (400 ml) and the organic layer was dried over Na₂SO₄. Solids were filtered off and volatiles were evaporated yielding 28 g (58 mmol, 89%) of the title compound as a light-brown solid. ¹H NMR (500 MHz, CDCl₃) δ 8.05 (d, *J* = 2.1 Hz, 1H), 7.70 (dd, *J* = 8.7, 2.2 Hz, 1H), 6.94 (d, *J* = 8.6 Hz, 1H), 4.31–4.20 (m, 3H), 3.96 (s, 3H), 2.87 (t, *J* = 12.9 Hz, 2H), 2.03 (apparent qd, *J* = 12.5, 4.5 Hz, 2H), 1.83–1.78 (m, 2H), 1.51 (s, 9H), 1.48 (s, 6H). LC-MS (ESI) *m/z* found: 424 (M + H, -t-Bu)⁺; retention time: 5.34 min. HRMS-ESI (M + H)⁺ calculated for C₂₂H₃₁N₃O₄: 480.1492, found: 480.1477.

Tert-butyl 4-(3-(4-methoxy-3-(pyridin-3-yl)phenyl)-4,4-dimethyl-5-oxo-4,5-dihydro-1H-pyrazol-1-yl)piperidine-1-carboxylate (40)

Boc-protected piperidine **39** (25.2 g, 52.5 mmol) and pyridin-3-ylboronic acid (9.0 g, 73 mmol) were charged to a round-bottom flask after which DME (400 ml) and 1 M Na₂CO₃ (210 ml, 210 mmol) were added. The mixture was degassed with N₂ for 15 m after which Pd (dppf) Cl₂ (2.1 g, 2.6 mmol) was added. The reaction was heated at 80°C for 16 h. The reaction mixture was diluted with MTBE (500 ml) and filtered over Celite. The residue was washed with saturated NaHCO₃ (2 ml × 600 ml) and brine (1 ml × 600 ml). The organic phase was dried over Na₂SO₄, filtered and concentrated *in vacuo* to yield 21.5 g (44.9 mmol, 86%) of the title compound. ¹H NMR (500 MHz, CDCl₃) δ 8.75

(s, 1H), 8.56 (d, $J = 4.0$ Hz, 1H), 7.84 (d, $J = 7.9$ Hz, 1H), 7.78 (d, $J = 2.0$ Hz, 1H), 7.75 (dd, $J = 8.6, 2.1$ Hz, 1H), 7.35 (dd, $J = 7.7, 4.9$ Hz, 1H), 7.01 (d, $J = 8.7$ Hz, 1H), 4.33–4.08 (m, 3H), 3.85 (s, 3H), 2.82 (s, 2H), 1.99 (apparent q, $J = 11.2$ Hz, 2H), 1.76 (d, $J = 11.6$ Hz, 2H), 1.47 (s, 7H), 1.45 (s, 9H). ^{13}C NMR (126 MHz, CDCl_3) δ 178.0, 161.2, 157.8, 154.7, 150.1, 148.3, 136.8, 133.5, 128.7, 127.7, 127.5, 124.0, 123.1, 111.1, 79.7, 55.8, 50.8, 48.8, 30.0, 28.4, 22.7. LC-MS (ESI) m/z found: 479 ($\text{M} + \text{H}$) $^+$; retention time: 4.03 min. HRMS-ESI ($\text{M} + \text{H}$) $^+$ calculated for $\text{C}_{27}\text{H}_{35}\text{N}_4\text{O}_4$: 479.2653, found: 479.2651.

3-(4-Methoxy-3-(pyridin-3-yl)phenyl)-4,4-dimethyl-1-(piperidin-4-yl)-1H-pyrazol-5(4H)-one Hydrochloride (41)

Boc-protected piperidine **40** (25.1 g, 52.4 mmol) was dissolved in dioxane (100 ml) and hydrogen chloride in dioxane (4 N) (131 ml, 524 mmol) was added in portions. The reaction was stirred for 40 h after which volatiles were evaporated. Attempts were made to recrystallize the resulting dark-oil from MTBE, *i*Pr-OH, *i*PrOH:H₂O to no avail. The crude was redissolved in EtOAc (800 ml) and extracted with aq. sat. Na_2CO_3 (2 ml \times 500 ml) and brine (500 ml). The organic layer was dried over Na_2SO_4 and volatiles were evaporated. Attempts to recrystallize from *i*-PrOH or *i*PrOH:H₂O were again unsuccessful. Evaporation of *i*-PrOH:H₂O ultimately yielded 16.7 g (44.1 mmol, 84%) of the title compound as a light brown powder. ^1H NMR (500 MHz, CDCl_3) δ 8.70–8.67 (m, 1H), 8.56 (dd, $J = 4.9, 1.6$ Hz, 1H), 7.91 (apparent dt, $J = 8.0, 1.9$ Hz, 1H), 7.85 (dd, $J = 8.7, 1.9$ Hz, 1H), 7.76 (d, $J = 1.8$ Hz, 1H), 7.47 (dd, $J = 7.7, 4.9$ Hz, 1H), 7.23 (d, $J = 8.8$ Hz, 1H), 4.08–3.96 (m, 1H), 3.84 (s, 3H), 3.00 (d, $J = 12.3$ Hz, 2H), 2.58–2.51 (m, 2H), 1.81 (apparent qd, $J = 12.3, 4.1$ Hz, 2H), 1.68–1.58 (m, 2H), 1.39 (s, 6H). ^{13}C NMR (126 MHz, CDCl_3) δ 177.2, 160.3, 157.5, 149.7, 149.6, 148.3, 148.2, 136.7, 133.2, 127.8, 127.2, 123.5, 123.4, 112.0, 55.9, 51.0, 48.0, 45.2, 31.2, 22.2. LC-MS (ESI) m/z found: 379 ($\text{M} + \text{H}$) $^+$; retention time: 2.40 min. HRMS-ESI ($\text{M} + \text{H}$) $^+$ calculated for $\text{C}_{22}\text{H}_{27}\text{N}_4\text{O}_2$: 379.2129, found: 379.2121.

1-(1-(cyclopropanecarbonyl)piperidin-4-yl)-3-(4-methoxy-3-(pyridin-3-yl)phenyl)-4,4-dimethyl-1H-pyrazol-5(4H)-one (42)

Amine **41** (100 mg, 0.26 mmol) was stirred with sodium hydride (60% in mineral oil) (16 mg, 0.40 mmol) in DMF (1 ml). After 30 min cyclopropanecarbonyl chloride (0.026 ml, 0.29 mmol) was added. The reaction was stirred for 2 h after which the reaction was quenched with water (20 ml) and extracted with EtOAc (20 ml). The organic layer was washed with sat. aq. NaHCO_3 solution (2 ml \times 20 ml), brine (20 ml) and dried over MgSO_4 . Volatiles were evaporated and the remaining crude was purified over SiO_2 using a gradient of 50% EtOAc in heptane toward 5% MeOH in EtOAc, yielding 45 mg (0.10 mmol, 38%) of the title compound as a white solid. ^1H NMR (500 MHz, CDCl_3) δ 8.78 (s, 1H), 8.60 (d, $J = 4.0$ Hz, 1H), 7.89 (d, $J = 7.9$ Hz, 1H), 7.80 (d, $J = 2.2$ Hz, 1H), 7.77 (dd, $J = 8.6, 2.2$ Hz, 1H), 7.41 (dd, $J = 7.7, 4.9$ Hz, 1H), 7.03 (d, $J = 8.7$ Hz, 1H), 4.75 (d, $J = 12.9$ Hz, 1H), 4.41–4.29 (m, 2H), 3.88 (s, 3H), 3.24 (t, $J = 12.7$ Hz, 1H), 2.72 (apparent t, $J = 12.4$ Hz, 1H), 2.14–1.74 (m, 7H), 1.50 (s, 6H), 1.05–0.95 (m, 2H), 0.77 (dd, $J = 7.9, 3.5$ Hz, 2H). ^{13}C NMR (126 MHz, CDCl_3) δ 178.0, 171.9, 161.3, 157.8, 149.8, 148.0, 137.2, 133.7, 128.7, 127.6, 127.5, 124.0, 123.3, 111.2, 55.8, 50.7, 48.8, 44.7, 41.4,

30.8, 29.7, 22.8, 11.1, 7.5, 7.4. LC-MS (ESI) m/z found: 447 ($\text{M} + \text{H}$) $^+$; retention time: 3.20 min. HRMS-ESI ($\text{M} + \text{H}$) $^+$ calculated for $\text{C}_{26}\text{H}_{31}\text{N}_4\text{O}_3$: 447.2391, found: 447.2390.

3-(4-Methoxy-3-(pyridin-3-yl)phenyl)-4,4-dimethyl-1-(1-(morpholine-4-carbonyl)piperidin-4-yl)-1H-pyrazol-5(4H)-one (83)

Amine **41** (400 mg, 1.1 mmol) was dissolved in dioxane (15 ml) and 25 ml of saturated NaHCO_3 was added followed by a dropwise addition of a 4-nitrophenyl chloroformate (639 mg, 3.2 mmol) in dioxane (10 ml) solution. The reaction mixture was stirred for 22 h, diluted with EtOAc and washed with a saturated sodium bicarbonate solution. The organic fraction was dried with brine, evaporated to dryness in the presence of SiO_2 and purified over the same medium using 1:3 EtOAc:hexane with 1% TEA toward 100% EtOAc with 1% TEA. After confirming identity of the product by semi-crude NMR it was used in the following step. K_2CO_3 (25 mg, 0.18 mmol) and morpholine (0.016 ml, 0.18 mmol) were dissolved in DMF (5 ml) to which the earlier isolated intermediate (50 mg, 0.092 mmol) was added. This reaction mixture was stirred at room temperature for 4 days and an additional equivalent morpholine (0.016 ml, 0.18 mmol) was added after 2 days. The reaction mixture was diluted with EtOAc (25 ml) and washed with sat. aq. Na_2CO_3 (25 ml). The aqueous layer was back extracted with EtOAc (25 ml) and the combined organic layers were washed with brine (25 ml), dried over Na_2SO_4 and concentrated *in vacuo*. The remaining crude was coated on SiO_2 and purified over SiO_2 using a gradient from EtOAc (1% TEA): cyclohexane 1:1 (v/v) toward 1% MeOH in EtOAc (1% TEA), evaporation of volatiles yielded a colourless oil which was redissolved in DCM and concentrated to afford 19 mg (0.039 mmol, 43%). ^1H NMR (600 MHz, CDCl_3) δ 8.83–8.78 (m, 1H), 8.62–8.59 (m, 1H), 8.04–7.98 (m, 1H), 7.82 (d, $J = 2.2$ Hz, 1H), 7.77 (dd, $J = 8.7, 2.2$ Hz, 1H), 7.49 (dd, $J = 7.8, 5.1$ Hz, 1H), 7.03 (d, $J = 8.7$ Hz, 1H), 4.29–4.23 (m, 1H), 3.87 (s, 3H), 3.85–3.80 (m, 2H), 3.70–3.63 (m, 4H), 3.31–3.25 (m, 4H), 2.94–2.83 (m, 2H), 2.10–2.02 (m, 2H), 1.85–1.78 (m, 2H), 1.49 (s, 6H). ^{13}C NMR (151 MHz, CDCl_3) δ 178.0, 163.9, 161.1, 157.8, 148.5, 146.5, 138.5, 134.4, 128.7, 128.0, 126.9, 124.2, 123.7, 111.2, 66.7, 55.8, 51.0, 48.8, 47.4, 46.1, 30.0, 22.7. LC-MS (ESI) m/z found: 492 ($\text{M} + \text{H}$) $^+$; retention time: 3.07 min. HRMS-ESI ($\text{M} + \text{H}$) $^+$ calculated for $\text{C}_{27}\text{H}_{34}\text{N}_5\text{O}_4$: 492.2605, found 492.2615.

DATA AVAILABILITY STATEMENT

The original contributions presented in the study are included in the article/Supplementary Material, further inquiries can be directed to the corresponding author.

AUTHOR CONTRIBUTIONS

MS contributed to the synthesis of the molecules, LM and GC did the parasitological screenings, MS, GS, IE, and RL were involved in the design of the molecules, LM, IE, and RL were responsible for obtaining the required funding, the manuscript was written by MS, GS, and RL and all authors made corrections and gave feedback to the manuscript.

FUNDING

The PDE4NPD project was funded by the European Union under the FP-7-Health program, project ID: 602,666.

REFERENCES

- Alpern, J. D., Lopez-Velez, R., and Stauffer, W. M. (2017). Access to Benznidazole for Chagas Disease in the United States—Cautious Optimism? *PLoS Negl. Trop. Dis.* 11, e0005794. doi:10.1371/journal.pntd.0005794
- Basore, K., Cheng, Y., Kushwaha, A. K., Nguyen, S. T., and Desai, S. A. (2015). How Do Antimalarial Drugs Reach Their Intracellular Targets? *Front. Pharmacol.* 6. doi:10.3389/fphar.2015.00091
- Batista, D. d. G. J., Batista, M. M., Oliveira, G. M. d., Amaral, P. B. d., Lannes-Vieira, J., Britto, C. C., et al. (2010). Arylimidamide DB766, a Potential Chemotherapeutic Candidate for Chagas' Disease Treatment. *Antimicrob. Agents Chemother.* 54, 2940–2952. doi:10.1128/aac.01617-09
- Bennion, B. J., Be, N. A., McNERney, M. W., Lao, V., Carlson, E. M., Valdez, C. A., et al. (2017). Predicting a Drug's Membrane Permeability: A Computational Model Validated with *In Vitro* Permeability Assay Data. *J. Phys. Chem. B* 121, 5228–5237. doi:10.1021/acs.jpcc.7b02914
- Bern, C. (2011). Antitrypanosomal Therapy for Chronic Chagas' Disease. *N. Engl. J. Med.* 364, 2527–2534. doi:10.1056/nejmct1014204
- Blaazer, A. R., Orrling, K. M., Shanmugham, A., Jansen, C., Maes, L., Edink, E., et al. (2014). Fragment-Based Screening in Tandem with Phenotypic Screening Provides Novel Antiparasitic Hits. *J. Biomol. Screen.* 20, 10. doi:10.1177/1087057114549735
- Castro, J. A., deMecca, M. M., and Bartel, L. C. (2006). Toxic Side Effects of Drugs Used to Treat Chagas' Disease (American Trypanosomiasis). *Hum. Exp. Toxicol.* 25, 471–479. doi:10.1191/0960327106het653oa
- Coura, J. R., and Borges-Pereira, J. (2011). Chronic Phase of Chagas Disease: Why Should it Be Treated? A Comprehensive Review. *Mem. Inst. Oswaldo Cruz* 106, 641–645. doi:10.1590/s0074-02762011000600001
- Coura, J. R., and Viñas, P. A. (2010). Chagas Disease: a New Worldwide Challenge. *Nature* 465, S6–S7. doi:10.1038/nature09221
- Dias, J. C. P. (1984). Acute Chagas' Disease. *Mem. Inst. Oswaldo Cruz* 79, 85–91. doi:10.1590/s0074-02761984000500017
- Hamers, R. L., Gool, T. V., Goorhuis, A., Cordeiro, M. A. S., Urbina, J. A., Gascon, J., et al. (2016). Benznidazole for Chronic Chagas' Cardiomyopathy. *N. Engl. J. Med.* 374, 189–190. doi:10.1056/NEJMc1514453
- Kollien, A., and Schaub, G. (2000). The Development of *Trypanosoma cruzi* in Triatominae. *Parasitol. Today* 16, 381–387. doi:10.1016/s0169-4758(00)01724-5
- Lidani, K. C. F., Andrade, F. A., Bavia, L., Damasceno, F. S., Beltrame, M. H., Messias-Reason, I. J., et al. (2019). Chagas Disease: From Discovery to a Worldwide Health Problem. *Front. Public Health* 7, 166. doi:10.3389/fpubh.2019.00166
- Martinez, F., Perna, E., Perrone, S. V., and Liprandi, A. S. (2019). Chagas Disease and Heart Failure: An Expanding Issue Worldwide. *Eur. Cardiol.* 14, 82–88. doi:10.15420/ecr.2018.30.2
- Meirelles, M. N., de Araujo-Jorge, T. C., Miranda, C. F., de Souza, W., and Barbosa, H. S. (1986). Interaction of *Trypanosoma cruzi* with Heart Muscle Cells: Ultrastructural and Cytochemical Analysis of Endocytic Vacuole Formation and Effect upon Myogenesis *In Vitro*. *Eur. J. Cell Biol* 41, 198–206.
- Mejia, A. M., Hall, B. S., Taylor, M. C., Gómez-Palacio, A., Wilkinson, S. R., Triana-Chávez, O., et al. (2012). Benznidazole-Resistance in *Trypanosoma cruzi* Is a Readily Acquired Trait that Can Arise Independently in a Single Population. *J. Infect. Dis.* 206, 220–228. doi:10.1093/infdis/jis331
- Morillo, C. A., Marin-Neto, J. A., Avezum, A., Sosa-Estani, S., Rassi, A., Rosas, F., et al. (2015). Randomized Trial of Benznidazole for Chronic Chagas' Cardiomyopathy. *N. Engl. J. Med.* 373, 1295–1306. doi:10.1056/nejmoa1507574
- Pinazo, M.-J., Guerrero, L., Posada, E., Rodríguez, E., Soy, D., and Gascon, J. (2013). Benznidazole-Related Adverse Drug Reactions and Their Relationship to Serum Drug Concentrations in Patients with Chronic Chagas Disease. *Antimicrob. Agents Chemother.* 57, 390–395. doi:10.1128/aac.01401-12
- Prata, A. (2001). Clinical and Epidemiological Aspects of Chagas Disease. *Lancet Infect. Dis.* 1, 92–100. doi:10.1016/s1473-3099(01)00065-2
- Rassi, A., Jr, Rassi, A., and Marin-Neto, J. A. (2010). Chagas Disease. *The Lancet* 375, 1388–1402. doi:10.1016/s0140-6736(10)60061-x
- Schmunis, G. A. (1999). Prevention of Transfusional *Trypanosoma cruzi* Infection in Latin America. *Mem. Inst. Oswaldo Cruz* 94, 93–101. doi:10.1590/s0074-02761999000700010
- Sgambatti de Andrade, A. L. S., Zicker, F., de Oliveira, R. M., Almeida e Silva, S., Luquetti, A., Travassos, L. R., et al. (1996). Randomised Trial of Efficacy of Benznidazole in Treatment of Early *Trypanosoma cruzi* Infection. *Lancet* 348, 1407–1413. doi:10.1016/s0140-6736(96)04128-1
- Sijm, M., Siciliano de Araújo, J., Kunz, S., Schroeder, S., Edink, E., Orrling, K. M., et al. (2019). Phenylidihydropyrazolones as Novel Lead Compounds against *Trypanosoma cruzi*. *ACS Omega* 4, 6585–6596. doi:10.1021/acsomega.8b02847
- Sijm, M., Sterk, G. J., Caljon, G., Maes, L., Esch, I. J. P., and Leurs, R. (2020). Structure-Activity Relationship of Phenylpyrazolones against *Trypanosoma cruzi*. *ChemMedChem* 15, 1310–1321. doi:10.1002/cmdc.202000136
- Torrico, F., Carlier, Y., Truyens, C., Suarez, E., Dramaix, M., Alonso-vega, C., et al. (2004). Maternal *Trypanosoma cruzi* Infection, Pregnancy Outcome, Morbidity, and Mortality of Congenitally Infected and Non-infected Newborns in Bolivia. *Am. J. Trop. Med. Hyg.* 70, 201–209. doi:10.4269/ajtmh.2004.70.201
- WHO (2021). Chagas Disease (American Trypanosomiasis). Available at: <http://www.who.int/mediacentre/factsheets/fs340/en/> (Accessed November 05, 2018).
- Zhang, L., and Tarleton, R. L. (1999). Parasite Persistence Correlates with Disease Severity and Localization in Chronic Chagas' Disease. *J. Infect. Dis.* 180, 480–486. doi:10.1086/314889

ACKNOWLEDGMENTS

Authors would like to thank D. Ahrens, A. Chen, M. Roseboom, J. Teeken H. Custers for technical assistance and M. Wijtmans for valuable advice.

- Conflict of Interest: The authors declare that the research was conducted in the absence of any commercial or financial relationships that could be construed as a potential conflict of interest.
- Copyright © 2021 Sijm, Maes, de Esch, Caljon, Sterk and Leurs. This is an open-access article distributed under the terms of the Creative Commons Attribution License (CC BY). The use, distribution or reproduction in other forums is permitted, provided the original author(s) and the copyright owner(s) are credited and that the original publication in this journal is cited, in accordance with accepted academic practice. No use, distribution or reproduction is permitted which does not comply with these terms.

GLOSSARY

ACN acetonitrile

AcOH acetic acid

BINAP 2,2'-bis(diphenylphosphino)-1,1'-binaphthyl

bs broad singlet

d days

d doublet

DBN 1,5-Diazabicyclo[4.3.0]non-5-ene

DCE dichloroethane

DCM dichloromethane

dd double doublet

DIPEA *N,N*-diisopropylethylamine

DMAP 4-dimethylaminopyridine

DME dimethoxyethane

DMF dimethylformamide

DMSO dimethylsulfoxide

dt double triplet

DTU discrete typing unit

EDCI 1-Ethyl-3-(3-dimethylaminopropyl)carbodiimide

ESI electron spray ionization

EtOAc ethylacetate

EtOH ethanol

FCS fetal calf serum

h heptethour

h heptethour

HOBt hydroxybenzotriazole

HPLC high pressure liquid chromatography

HRMS high resolution mass spectroscopy

Hz Hertz

i-PrOH isopropanol

LC-MS liquid chromatography mass spectroscopy

m minute

m multiplet

MeOH methanol

MRC-5 medical research council strain 5

MTBE methyl tertbutyl ether

NaOtBu sodium tert-butoxide

o.n. overnight

p pentet

PDE4NP phosphodiesterase inhibitors for neglected parasitic disease

pIC₅₀ -log of the value at which 50% of growth is inhibited

rt room temperature

s singlet

SAR structure activity relationship

t triplet

T3P propylphosphonic anhydride

Tcr *Trypanosoma cruzi*

TEA triethylamine

q quartet

THF tetrahydrofuran

TLC thin layer chromatography

UV ultraviolet